International Journal of Heat and Mass Transfer 52 (2009) 2407–2414

Contents lists available at ScienceDirect

International Journal of Heat and Mass Transfer

journal homepage: www.elsevier.com/locate/ijhmt

Analytical determination of viscous permeability of fibrous porous media

A. Tamayol *, M. Bahrami

Mechatronic Systems Engineering, School of Engineering Science, Simon Fraser University, Surrey, BC, Canada V3T0A3

A R T I C L E I N F O

Article history:
Received 22 April 2008
Received in revised form 11 September 2008
Available online 12 January 2009

Keywords:
Fibrous media
Permeability
Integral technique
Unit cell
Analytical solution
Modeling

A B S T R A C T

In this study, the permeability of ordered fibrous media towards normal and parallel flow is determined analytically. In this approach, porous material is represented by a "unit cell" which is assumed to be repeated throughout the media. Several fiber arrangements including: touching and non-touching arrays are considered. Modeling 1D touching fibers as a combination of channel-like conduits, a compact relationship is proposed to predict permeability. Furthermore, employing an "integral technique" and assuming a parabolic velocity profile within the unit cells, analytical relationships are developed for pressure drop and permeability of rectangular arrangements. The developed models are successfully verified with existing experimental data collected by others for square arrangement over a wide range of porosity. Due to the random nature of the porous micro structures, determination of exact permeability of real fibrous media is impossible. However, the analyses developed for ordered unit cells enable one to predict the trends observed in experimental data. The effects of unit cell aspect ratio and fibers diameter on the permeability are also investigated. It is noted that with an increase in the aspect ratio the normal permeability decreases while, the parallel permeability remains constant. It is also shown that the permeability of fibrous media is related to the diameter of fibers squared.

1. Introduction

Fibrous porous materials have applications in several engineering areas including: filtration and separation of particles, physiological systems, composite fabrication, heat exchangers, thermal insulations, and fuel cells [1–4]. Transport phenomena in porous media have been the focus of numerous studies since 1940s which indicates the importance of this topic. One of the most important properties of porous structures is permeability. Permeability is a measure of the ability of porous matrix to transport fluids. Prediction of velocity field plays a key role in estimating permeability and analyzing the flow behavior in porous media. This can be achieved by using Darcy's law which assumes a linear relationship between volume-averaged superficial fluid velocity, $\overline{U}$, and the pressure gradient:

$$-\nabla P = \frac{\mu}{K}\overline{U} \tag{1}$$

where μ is the fluid viscosity and K is the permeability of the medium. Darcy's relationship is empirical, convenient, and widely accepted. It can be shown that Darcy's equation holds while fluid flowing through pores is in creeping regime [5]. To use Darcy's equation; however, we need to know the permeability of the medium beforehand. Permeability depends on several factors, including: porosity, fibers size distribution, and arrangement; it is typically found using empirical correlations for most applications.

Prediction of the permeability of fibrous media dates back to experimental work of Sullivan in 1940s [6] and theoretical works of Kuwabara [7], Hasimoto [8], Happel [9], and Sparrow and Loeffler [10] in 1950s. Kuwabara [7] predicted the permeability of flow normal to randomly arranged fibers for materials with high porosity. He solved the stream function and the vorticity transport equations around with limited boundary layer approach. Hasimoto [8] and Sparrow and Loeffler [10] determined the permeability of normal and parallel flow to ordered arrangement of cylinders, respectively. Happel [9] analytically solved the Stoke's equation for parallel and normal flow to a single cylinder with free surface model (limited boundary layer). He also proposed that the permeability of random fibrous media is related to parallel and normal permeability of 1D array of cylinders. Later, Sangani and Acrivos [11], performed analytical and numerical studies of viscous permeability of square and staggered arrays of cylinders for the entire range of porosity, while their axes were perpendicular to the flow direction. Their analytical models were accurate for lower and higher limits of porosity. Sangani and Yao [12] reported numerical results for the permeability of random 1D fibers towards normal and parallel flows. Sahraoui and Kaviany [13] included inertial effects and numerically determined the permeability of cylinders in normal flow and proposed a correlation. Van der Westhuizen and Du Plessis [14] using numerical simulations proposed a correlation for prediction of normal permeability of 1D fibers. Analytical

* Corresponding author.
E-mail addresses: ata42@sfu.ca (A. Tamayol), mbahrami@sfu.ca (M. Bahrami).

0017-9310/$ - see front matter © 2008 Elsevier Ltd. All rights reserved.
doi:10.1016/j.ijheatmasstransfer.2008.09.032

Nomenclature

A	pore cross-sectional area (normal to flow), m^2
d	fiber diameter, m
D_h	hydraulic diameter of the pore, m
f	Fanning friction coefficient
I_p	polar moment of inertia of pore cross-section, m^4
I_p^*	dimensionless polar moment of inertia of pore cross-section, $I_p^* = I_p/A^2$
K	permeability, m^2
K^*	non-dimensional permeability, $K^* = K/d^2$
L	channel depth, m
P	pressure, N/m^2
Q	volumetric flow rate, m^3/s
S	distance between adjacent fibers in square arrangement, m
S_x	distance between adjacent fibers in rectangular unit cell in x-direction, m
S_y	distance between adjacent fibers in rectangular unit cell in y-direction, m
u	normal velocity, m/s
u_s	velocity at the border of unit cell, m/s
$\bar{U}$	volume-averaged superficial velocity, m/s
w	parallel velocity, m/s
Greek symbols	
Γ	perimeter of flow passages, m
ε	porosity
μ	viscosity, N s/m^2
φ	solid fraction, $\varphi = 1 - \varepsilon$
φ'	non-dimensional parameter, $\varphi' = \pi/4\varphi$
Subscript	
D-W	Darcy–Weisbach

prediction of the permeability of general triangular arrangement was presented by Hellou et al. [15]. They proposed a correlation for determination of permeability of periodic triangular arrangements. Recently, Sobera and Kleijn [16] studied the permeability of random 1D and 2D fibrous media both analytically and numerically. Their analytical model was based on scale analysis and the proposed relationship was a function of fibers distance and a non-dimensional randomness number. A comparison of model of [16] with numerical results showed that their model was accurate in highly porous materials [16]. However, the difference in low porosity was considerable. Tomadakis and Sotirchos [17] proposed a model which enables the prediction of anisotropic permeability through 1D, 2D, and 3D random fibrous beds. This model was proposed for randomly overlapping fibers. Although model of [17] were meant to cover all types of random fibrous media, in some cases the errors between the model and experimental data were considerable. A thorough comparison of [17] model with experimental data, is available in [2]. Avellaneda and Torquato [18] using conduction-based techniques, proposed an upper bound for the permeability of generalized fibrous media. Tomadakis and Robertson [2] showed that this bound is violated by several data points available in the literature. Using experimental data, Tomadakis and Robertson [2] stated that the upper and lower bounds for fibrous media with random orientation of fibers were normal and parallel permeability of 1D arrangements. Several experimental studies have also been conducted for determination of the permeability of fibrous media [19–25]. Good reviews of experimental works are available in Jackson and James [26], Astrom et al. [27], and Tomadakis and Robertson [2].

Porous media have potential applications in compact heat exchangers and fuel cell technologies. Our literature review indicates that less attention has been paid to determination of permeability of ordered packed fibrous materials. More importantly, we observed that: (1) majority of the existing correlations for permeability are based on curve-fitting of experimental or numerical data; (2) most of the analytical models found in the literature are not general and fail to predict permeability over the entire range of porosity.

In this study, the permeability of touching and non-touching ordered fibrous media towards normal and parallel flow is studied. A compact relationship is presented that can be used for touching fibers and also packed beds.

In addition, novel analytical models are developed using the concept of unit cell and integral technique. Assuming a parabolic velocity profile within the unit cells and integrating the continuity and momentum equations, compact analytical relationships are derived for pressure drop and permeability of considered patterns. Using the proposed model, one only needs average fibers diameter and the medium porosity to predict the permeability. More importantly, the present analysis does not require any tuning parameters. Normal and parallel permeability of 1D fibrous media are studied to establish bounds, as previously pointed out by Tomadakis and Robertson [2]. It is shown that the proposed normal flow permeability of square unit cell predicts the trends observed in experimental data; and serves as a lower bound for the permeability of fibrous media. The proposed model is successfully validated against experimental data collected from several sources over a wide range of porosity, matrix materials, and fluids.

2. Model development

Due to the random nature of porous micro structures, determination of exact permeability of real fibrous media is highly unlikely. As a result, simplifying assumptions should be made to model the geometry of the microstructure. Fibrous media can be categorized into three forms [2]:

(1) One dimensional (1D): fibers are parallel to each other but, randomly distributed in the volume.
(2) Two dimensional (2D): fibers are located in parallel planes in which the fibers can have random orientation.
(3) Three dimensional (3D): fibers can have any orientations and locations in the space.

Among the above three types, the 1D model is the most anisotropic type and is considered in this study. Following the approach used successfully in several applications such as spherical packed beds [28] and in gas diffusion layer of fuel cells [29], and fibrous media [7–11,30,31] a unit cell is considered to analyze the geometry of the fibrous media. The unit cell (or the basic cell) is the smallest volume which can represent characteristics of the whole microstructure. Porous media are assumed to be periodic and the considered unit cells repeat throughout the material. In the following sections several fiber arrangements including: touching and non-touching arrays are considered. The flow is assumed to be creeping, incompressible and steady state.

Determination of the exact velocity profile requires detail knowledge of the geometry of the medium which is not feasible in the case of porous media. Moreover, even with specified geometry and boundary conditions, finding exact analytical solution is not guaranteed and is a difficult task for most cases. To overcome this problem, an integral method is employed in this study. The integral method provides a powerful technique for obtaining accurate but approximate solutions to rather complex problems with remarkable ease. The basic idea is that we assume a general shape of the velocity profile. It must be noted that we are not interested in the precise shape of velocity profile but rather need to know the pressure drop over the basic cell to calculate permeability. This can be accomplished by satisfying conservation of mass and momentum in a lumped fashion across the unit cell. As a result, an approximate parabolic velocity profile is considered which satisfies the boundary conditions within the unit cell. The integral technique has been applied successfully to several classical problems such as moving plate and boundary layer [32]. Use this technique to model porous media, however, is a novel approach. In the following sections, a combination of integral technique and asymptotic solution are undertaken to study the flow in a variety of fiber arrangements.

3. Permeability of touching fibers

Two limits can be recognized for fibrous media:

(1) Touching cylinders, media can be envisioned as a packed bed.
(2) Highly porous materials with porosities near 1.

Although packed fibrous beds have application in compact heat exchangers, most of the proposed models and analytical solutions existing in the literature fail to predict the permeability of these materials [24].

Since no flow could pass perpendicular to touching fibers (see figures in Table 1), normal permeability is zero. Fluid passing parallel to the axis of unidirectional fibers experiences a channel-like flow; thus, the media is treated as a combination of parallel constant cross-sectional conduits. Therefore, the permeability can be related to pressure drop in these channel flows. In this approach, the cross-sectional area and the perimeter of the channel are required. Pressure drop can be calculated using Darcy–Weisbach relation [32]:

$$\frac{dP}{dz} \approx \frac{\Delta P}{L} = f\,\frac{\rho \overline{U}^2}{2\varepsilon^2 D_h} \qquad (2)$$

where D_h is the hydraulic diameter, L is the channel depth, f is the Fanning friction factor, and ε and $\overline{U}$ represent the porosity and the volume-averaged superficial velocity, respectively. Using Eq. (1) the permeability becomes:

$$K_{D-W} = f\,\frac{2\varepsilon^2 \mu D_h}{f \rho \overline{U}} \qquad (3)$$

Table 1 presents several touching fibers arrangements and the calculated permeability using Eq. (3). Note that the Fanning friction factor must be known to calculate permeability from Eq. (3). Numerical values of the Fanning coefficients reported by Shah and London [33] and the resulted permeabilities are also listed in Table 1. It should be noted that all of these possible arrangements cannot be considered as a unit cell. Fig. 1a–c shows how the triangular, the rectangular, and the hexagonal arrangements can map a porous medium; As a result, they are unit cells. However, the octagonal arrangement in Table 1 does not represent, by itself, the characteristics of the fibrous media since it must be combined by the rectangular arrangement.

Selection of the characteristic length is an arbitrary choice and will not affect the final solution. However, a more appropriate length scale leads to more consistent results, especially when random cross-sections are considered such as in porous media. A

Table 1
Touching parallel fibers parameters.

Porosity (ε)	Arrangement shape	f Ref.[33]	D_h	K_{D-W}/d^2, Eq. (3)
0.094	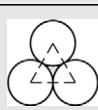	6.503	$0.103d$[1]	0.00008
0.215	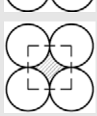	6.606	$0.274d$	0.00122
0.316	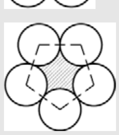	6.634	$0.462d$	0.00509
0.396	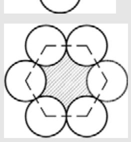	6.639	$0.655d$	0.01280
0.512	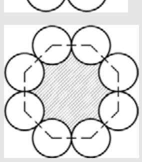	6.629	$1.050d$	0.04260

Normal flow permeability = 0 for these arrangements.
[1] d is the fibers diameter.

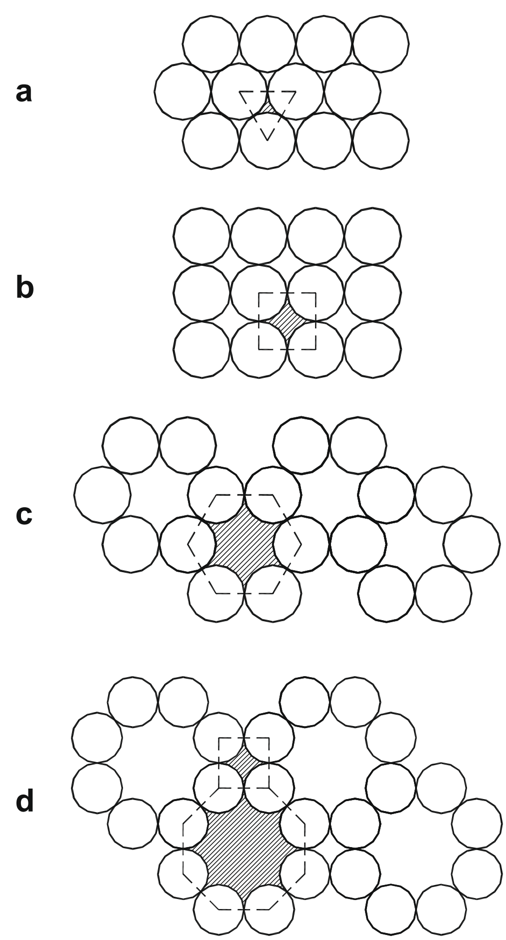

Fig. 1. Triangular, square, and hexagonal unit cells and combination of octagonal and square array of cylinders.

circular duct is fully described with its diameter, thus the obvious length scale is the diameter (or radius). For non-circular cross-sections, the selection is not as clear; many textbooks and researchers have conventionally chosen the hydraulic diameter. Yovanovich [34,35] introduced the square root of area ($\sqrt{A}$) as a characteristic length scale for heat conduction and convection problems. Bahrami et al. [36,37] through analysis showed that $\sqrt{A}$ appears in the solution of fully-developed flow in non-circular ducts. They also compared both D_h and $\sqrt{A}$ and observed that using $\sqrt{A}$ as the characteristic length scale results in similar trends in Poiseuille number for microchannels with a wide variety of cross-sections. Therefore, in this study, the Fanning friction coefficient is calculated employing Bahrami et al. [36] model which considered $\sqrt{A}$ as the length scale. They proposed a general model that predicts the pressure drop for arbitrary cross-sectional channels. In the model of [36], pressure drop is related to geometrical parameters of the cross-section:

$$\frac{\Delta P}{L} = \frac{16\pi^2 \mu \overline{U}}{A\varepsilon} I_p^*, \qquad I_p^* = \frac{I_p}{A^2} \tag{4}$$

where I_p and A are the polar moment of inertia and the area of the passage cross-section, respectively. Using Darcy's relationship and model of [36], the non-dimensional permeability of periodic touching fibrous media can be found as:

$$K^* = \frac{K}{d^2} = \frac{A\varepsilon}{16\pi^2 I_p^*} \tag{5}$$

This relationship can be easily applied to any touching fibrous arrangements including; triangular, rectangular, hexagonal, and checker boarding. Table 2 compares the values calculated from Eq. (5) and the experimental data reported by Sullivan [6] for air flowing through staggered and square arrangements of copper wires, respectively. The difference between the predicted values by the proposed model and the experimental data is reasonably within the context of porous media.

4. Normal permeability of square arrangement

Fig. 2 shows the rectangular arrangement of cylinders and the velocity profile between these fibers. The unit cell is selected as the space between parallel cylinders as shown in this figure. For convenience and without losing generality, the unit cell is assumed to be square, i.e., $S_x = S_y = S$. The same approach can be followed for the rectangular unit cell. The porosity for this arrangement can be determined from:

$$\varepsilon = 1 - \frac{\pi d^2}{4S^2} \tag{6}$$

The permeability is related to the total pressure drop through the unit cell; see Eq. (1). Assuming creeping flow and neglecting inertial terms, the x-momentum equation reduces to Stokes equation:

Table 2
Parallel permeability of touching fibers.

Porosity (ε)	Unit cell	K^*, Eq. (5)	K^*, data [6]	Difference (%)
0.094	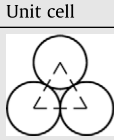	0.000088	0.000083	5.6
0.215	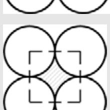	0.00147	0.00121	17.6

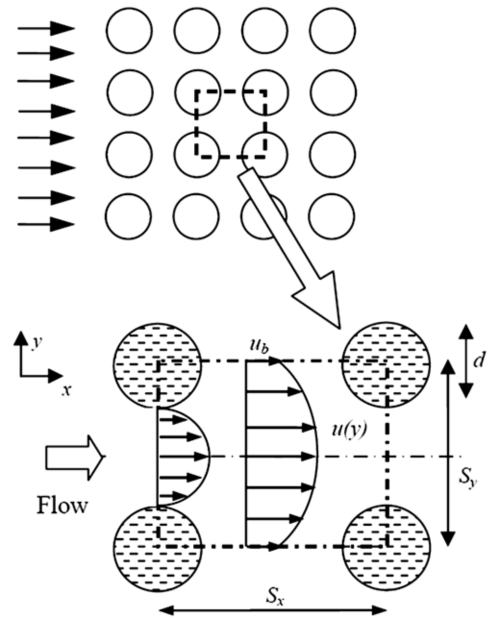

Fig. 2. Rectangular arrangement of cylinders and considered unit cell.

$$\frac{\partial^2 u}{\partial y^2} = \frac{1}{\mu}\frac{dP}{dx} \tag{7}$$

Due to symmetry, the y-component of velocity on the unit cell border line is zero. The x-component of velocity is not necessarily zero; however, for very packed materials the border velocity is negligible. At first, no border velocity assumption is made to simplify the analysis. Later, the effect of the border velocity on porosity will be investigated. Solving Eq. (7) and assuming no-slip condition leads to a parabolic velocity profile:

$$u = \frac{1}{2\mu}\frac{dP}{dx}(\delta^2 - y^2) \tag{8}$$

where δ is the half thickness of the unit cell in y-direction. For the unit cell of the rectangular arrangement, Fig. 2b, δ is:

$$\delta = \begin{cases} \frac{S}{2} - \sqrt{\frac{d^2}{4} - x^2}, & 0 \leqslant x \leqslant \frac{d}{2} \\ \frac{S}{2}, & \frac{d}{2} \leqslant x \leqslant \frac{S}{2} \end{cases} \tag{9}$$

Total pressure drop of the unit cell is calculated employing an integral technique solution. Substituting velocity profile of Eq. (8) into continuity equation and integrating the result, the unit cell pressure drop is calculated:

$$\Delta P_{unitcell} = 3\mu Q \int_0^{S/2} \frac{dx}{\delta^3} \tag{10}$$

where $Q = \overline{U}S$ is the total volumetric flow rate passing through the unit cell. The pressure drop in the basic cell is calculated as:

$$\Delta P_{unitcell} = 6\mu Q \left\{ \frac{2d}{(S^2 - d^2)S} + \frac{3d^2 S\left[\tan^{-1}\left(\frac{d}{\sqrt{S^2-d^2}}\right) + \frac{\pi}{2}\right]}{(S^2 - d^2)^{\frac{5}{2}}} \right\} + \frac{12\mu Q}{S^3}(S - d) \tag{11}$$

Using the total pressure drop over the length of the unit cell, one can rewrite Darcy's relation as:

$$\frac{\Delta P_{unitcell}}{S} = \frac{\mu Q}{KS} \tag{12}$$

Combining Eqs. (11) and (12), one can observe that the permeability is only a function of the geometrical parameters of the media, which is in line with the creeping flow assumption. Introducing solid fraction as $\phi = 1 - \varepsilon$, the permeability of square arrangement becomes:

$$K^* = \left\{ \frac{12\left(\sqrt{\phi'}-1\right)}{\phi'\sqrt{\phi'}} + \frac{18+12(\phi'-1)}{\sqrt{\phi'}(1-\phi')^2} + \frac{18\sqrt{\phi'}\left[\tan^{-1}\left(\frac{1}{\sqrt{\phi'-1}}\right)+\frac{\pi}{2}\right]}{(\phi'-1)^{\frac{5}{2}}} \right\}^{-1} \quad (13)$$

where $K^* = K/d^2$ and $\phi' = \pi/4\phi$. Eq. (13) is based on the assumption of no border velocity, i.e., $u_b = 0$. In general, the border velocity is not zero. It is zero on the edge of the cylinders (no-slip condition) and reaches its maximum value at the half distance between cylinders in the x-direction. It is also expected that the maximum border velocity be a function of the porosity [21], i.e., as the porosity increases the maximum border velocity increases. For lower porosities the border velocity is very small and for highly porous limits, approaches to the Darcy velocity. In this study, the border velocity increases linearly from the edge of the fibers ($u_b = 0$) to its peak at the center of the unit cell:

$$u_b = \overline{U} g(\varepsilon) \frac{2x}{S-d}, \quad \frac{d}{2} \leqslant x \leqslant \frac{S}{2} \quad (14)$$

In Eq. (14) the maximum border velocity is related to porosity through $g(\varepsilon)$ which is assumed to be a linear function of porosity; with $g(0.215) = 0$ for touching fibers and $g(1) = 1$ for high porosity limits:

$$g(\varepsilon) = 1.274\varepsilon - 0.274 \quad (15)$$

Using Eq. (14), our model can be extended to account for the border velocity. Since the no-slip boundary condition holds for the fibers surface, the velocity profile in Eq. (8) is valid for $0 \leqslant x \leqslant d/2$ range. But, for $d/2 \leqslant x \leqslant s/2$, the velocity profile becomes:

$$u = \frac{1}{2\mu}\frac{dP}{dx}\left(\frac{S^2}{4} - y^2\right) + g(\varepsilon)\frac{2x}{S-d}\overline{U}, \quad \frac{d}{2} \leqslant x \leqslant \frac{S}{2} \quad (16)$$

Using continuity equation and the definition of volumetric flow rate, one can calculate pressure gradient:

$$\frac{dP}{dx} = \frac{12\mu Q}{S^3}(S-d)\left[1 - g(\varepsilon)\frac{2x}{S-d}\right], \quad \frac{d}{2} \leqslant x \leqslant \frac{S}{2} \quad (17)$$

The pressure drop in the basic cell is calculated as:

$$\Delta P_{unitcell} = 6\mu Q \left\{ \frac{2d}{(S^2-d^2)S} + \frac{3d^2 S\left[\tan^{-1}\left(\frac{d}{\sqrt{S^2-d^2}}\right) + \frac{\pi}{2}\right]}{\left(S^2 - d^{2\frac{5}{2}}\right)} \right\} + \frac{12\mu Q}{S^3}(S-d)\left[\frac{2-g(\varepsilon)}{2}\right] \quad (18)$$

Following the same approach, the permeability of the square arrangement can be determined as:

$$K^* = \left\{ \frac{12(\sqrt{\pi'}-1)}{\phi'\sqrt{\phi'}}\left[\frac{2-g(\varepsilon)}{2}\right] + \frac{18+12(\phi'-1)}{\sqrt{\phi'}(1-\phi')^2} + \frac{18\sqrt{\phi'}\left[\tan^{-1}\left(\frac{1}{\sqrt{\phi'-1}}\right)\right]}{(\phi'-1)^{\frac{5}{2}}} \right\}^{-1} \quad (19)$$

In Fig. 3 predicted results from the present models, Eqs. (13) and (19) are compared with experimental data collected from several sources. The ±15% bounds of the model are also shown in the

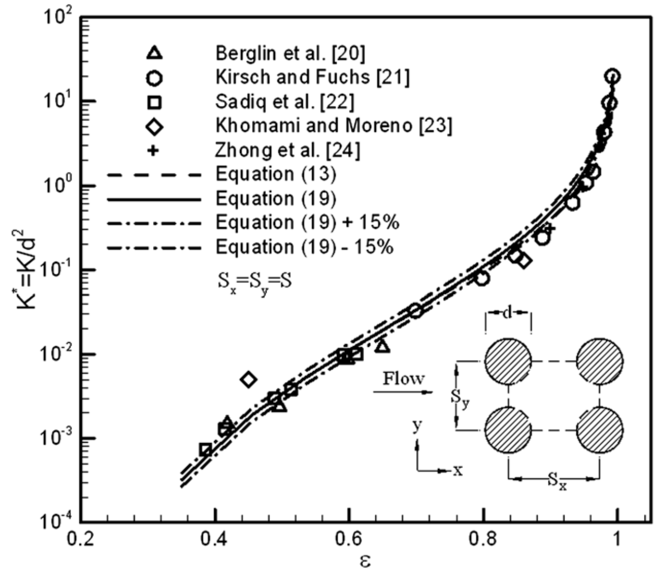

Fig. 3. Comparison of present models with experimental data.

plot, to better demonstrate the agreement between the data and the model. The experiments were conducted using different fluids including: air, water, oil, and glycerol with a variety of porous materials such as metallic rods, glass wool, and carbon. As expected, the difference due to neglecting the border velocity is only considerable in highly porous materials. More importantly, the proposed model, Eq. (19), accurately predicts the normal permeability of square arrangement of fibers over the entire range of porosity.

A comparison between Eq. (19), experimental data, and other existing models is also presented in Fig. 4. Although most of the models predict similar trends for porosities near unity, they fail to predict the data for low porosities. The proposed model, on the other hand, is the only analytical-based model that captures the trends of experimental data over the entire range of porosity; and does not include any unknown constants.

According to Tomadakis and Robertson [2], values for flow normal and parallel to 1D fiber arrangement present the lower and upper bounds for the permeability of fibrous media. Sobera and

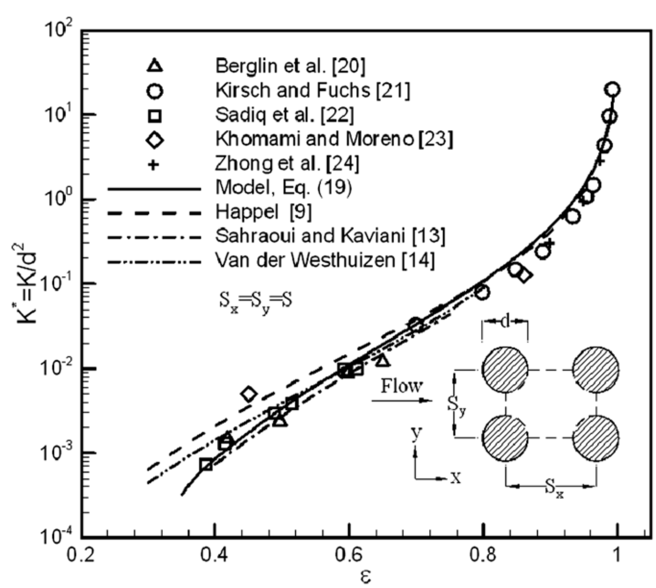

Fig. 4. Comparison between proposed model, experimental data, and other existing models.

Kleijn [16] also showed that among all possible 1D arrangements, repeating pattern of Fig. 2 has the minimum permeability. Therefore, Eq. (19) can serve as a lower bound for the permeability of random fibrous media.

5. Parallel permeability of square arrangement

For this arrangement, the selected unit cell is the space between parallel cylinders as shown in Fig. 5. The fluid flows perpendicular to paper. Following the same approach discussed in the previous section, a parabolic velocity profile is assumed:

$$w = \frac{1}{2\mu}\frac{dP}{dz}(\delta^2 - y^2), \quad 0 \leqslant x \leqslant \frac{d}{2} \tag{20}$$

$$w = \frac{1}{2\mu}\frac{dP}{dz}\left(\left(\frac{S}{2}\right)^2 + \left(\frac{S-d}{2}\right)^2 - \left(x - \frac{S}{2}\right)^2 - y^2\right), \quad \frac{d}{2} \leqslant x \leqslant \frac{S}{2}$$

where w is the velocity parallel to fibers in the z-direction, and δ is defined by Eq. (9). Using the continuity equation, one can calculate the volumetric flow rate through the unit cell as:

$$Q = \int\int_{A_{unitcell}} w\,dy\,dx \tag{21}$$

which can be evaluated as:

$$Q = \frac{1}{6\mu}\frac{dP}{dz}\left[\left(S^2 + 3d^2\right)\frac{Sd}{2} - \frac{Sd^3}{2} - \frac{3\pi}{32}\left(4S^2 + d^2\right) + \frac{S(S-d)^3}{2} + \frac{S^4}{2}\right] \tag{22}$$

Using Darcy's relationship and substituting for Q from the above, one can find the parallel permeability:

$$K^* = \left\{\frac{\pi}{24\phi} + \left[\left(\sqrt{\frac{\pi}{4\phi}} - 1\right)^3 + 2\right]\sqrt{\frac{\phi}{9\pi} - \left(\frac{\pi}{8} + \frac{\phi}{8}\right)}\right\}\frac{1-\phi}{2} \tag{23}$$

The present model, Eq. (23), is compared with analytical model of Happel [9], numerical results of Sangani and Yao [12], and experimental data reported by Sullivan [6] and Skartsis and Kardos [23] for flow parallel to square arrangements of fibers, in Fig. 6. The analytical model of [9] is accurate for high porosities [5]. This figure indicates that the proposed model shows a better agreement with experimental data in low porosities.

6. Effects of unit cell aspect ratio

After successfully validating the proposed model, we can now use it to investigate the effect of major parameters. Effects of porosity have already been discussed in the previous sections. Eqs. (19) and (23) indicate that permeability is directly related to fibers diameter squared for square arrangement.

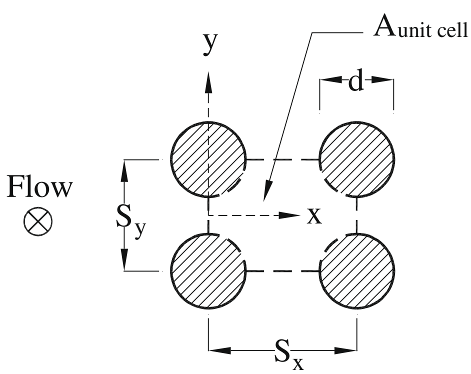

Fig. 5. Parallel flow through rectangular unit cell.

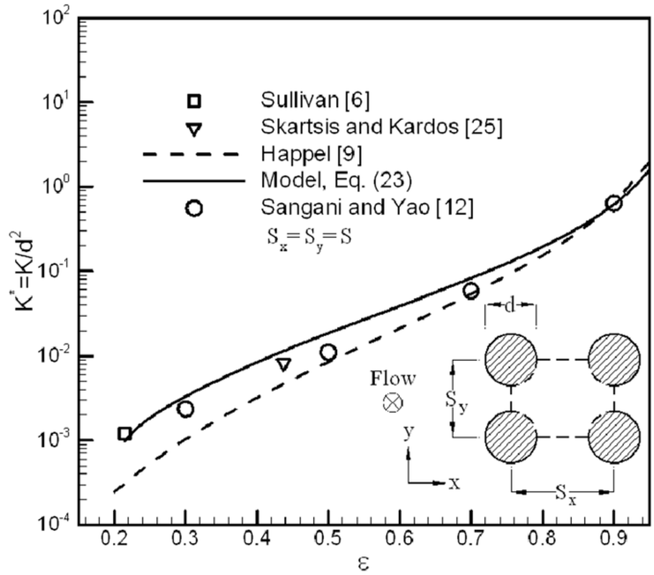

Fig. 6. Comparison of present model for parallel permeability of square arrangement with experimental data of [6] and [23] and analytical model of Happel [9].

Although Eqs. (19) and (23) are presented for square arrangement, the same analysis can be followed to study the effects of unit cell aspect ratio, S_x/S_y, variation on the non-dimensional permeability of normal flow through rectangular fibers arrangement. In Fig. 7a the non-dimensional permeability, K^*, is plotted versus unit cell aspect ratio for normal and parallel flow through rectangular cell. Porosity and fibers diameter are kept constant while aspect ratio is varied. The range of aspect ratio is determined by the non-overlapping constraint for fibers, i.e., $S_x, S_y \geqslant d$. For example, for $\varepsilon = 0.5$ the range of unit cell aspect ratio will be $0.636 \leqslant S_x/S_y \leqslant 1.572$.

Fig. 7a shows that normal permeability decreases as unit cell aspect ratio is increased. This is a direct result of reduction of the distance between adjacent fibers normal to the flow direction. For relatively low porosities the variation of permeability is considerable; however, for highly porous materials this variation is relatively small.

The non-dimensional permeability is plotted against unit cell aspect ratio in Fig. 7b for parallel flow in rectangular cell. The changes of parallel permeability due to the variation of aspect ratio are not as significant as the values of normal flow. It should be noted that 1D fibers parallel to the flow can be treated as capillaries with slip velocity boundary condition; therefore, the permeability in this case is related to the cross-section of the pores. Since the area of the unit cell is not changing while porosity is kept constant, the parallel permeability is not considerably affected by the variation of basic cell aspect ratio.

7. Summary and conclusions

The permeability of ordered fibrous media towards normal and parallel flow is analyzed. In this study, porous material is represented by a unit cell which is assumed to be repeated throughout the media. Several fiber arrangements including: touching and non-touching arrays are considered. Modeling parallel touching fibers as a combination of channel-like passages, a compact relationship is proposed for prediction of the permeability. Analytical models are also developed by using the concept of unit cell and

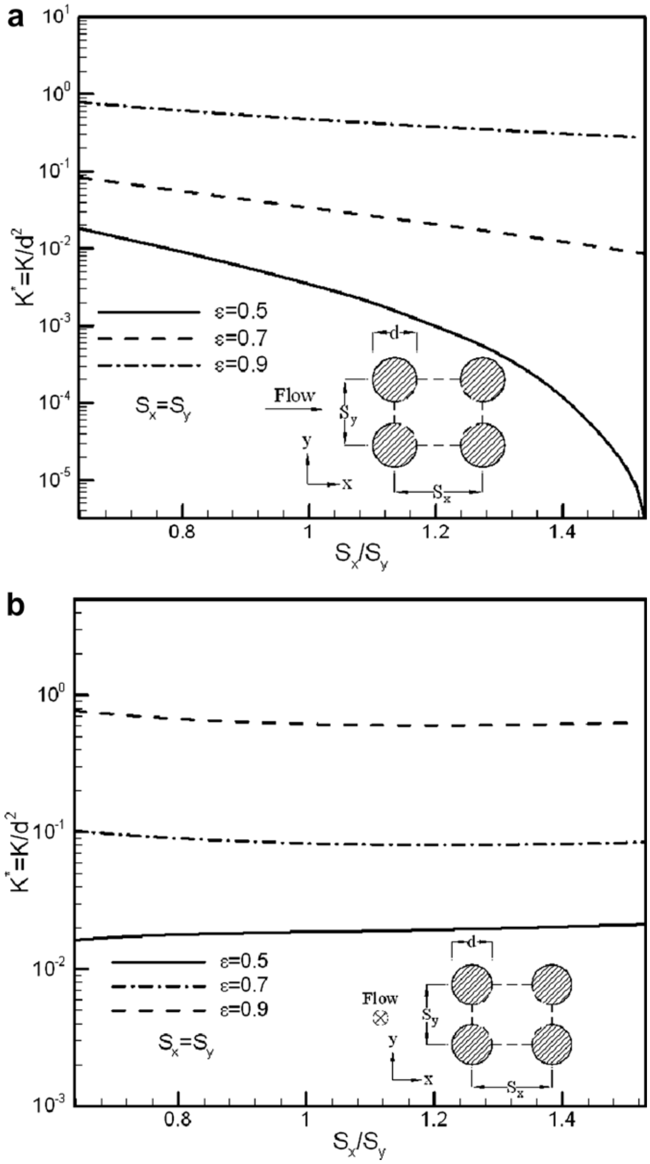

Fig. 7. Non-dimensional permeability versus unit cell aspect ratio for (a) normal, (b) parallel flow through square arrangement.

introducing an integral technique solution. Assuming a parabolic velocity profile within the unit cells, analytical relationships are developed for pressure drop and permeability of considered patterns. The proposed model only requires the fibers diameter and the medium porosity, with no constant or parameter, to predict the permeability of fibrous media. The developed models have been successfully compared with experimental data collected from different sources as well as existing models in the literature for square arrangement over a wide range of porosity. It is also shown that the proposed normal flow permeability of square unit cell serves as a lower bound for the permeability of fibrous media.

A parametric study was conducted and highlights of the analysis were:

- The permeability is a function of geometrical parameters such as: porosity, fiber diameter and unit cell aspect ratio in case of rectangular fibers arrangement.
- Normal and parallel permeability are directly related to the fiber diameter squared.

The present analysis provides an in-depth knowledge on the effects of geometrical and thermophysical parameters involved on the permeability of fibrous media. This information can be used as guidelines and criteria to design, select, and optimize engineering systems that include porous media.

Acknowledgments

The authors gratefully acknowledge the financial support of the Natural Sciences and Engineering Research Council of Canada, (NSERC).

References

[1] D.S. Clauge, R.J. Philips, A numerical calculation of the hydraulic permeability of three-dimensional disordered fibrous media, Phys. Fluids 9 (6) (1997) 1562–1572.
[2] M.M. Tomadakis, T. Robertson, Viscous permeability of random fiber structures: comparison of electrical and diffusion estimates with experimental and analytical results, J. Compos. Materials 39 (2005) 163–188.
[3] J.T. Gostick, M.W. Fowler, M.D. Pritzker, M.A. Ioannidis, L.M. Behra, In-plane and through-plane gas permeability of carbon fiber electrode backing layers, J. Power Sources 162 (2006) 228–238.
[4] J.P. Feser, A.K. Prasad, S.G. Advani, Experimental characterization of in-plane permeability of gas diffusion layers, J. Power Sources 162 (2006) 1226–1231.
[5] M. Kaviany, Principles of Heat Transfer in Porous Media, Springer-Verlag, New York, 1992.
[6] R.R. Sullivan, Specific surface measurements on compact bundles of parallel fibers, J. Appl. Phys. 13 (1942) 725–730.
[7] S. Kuwabara, The forces experienced by randomly distributed parallel circular cylinders or spheres in a viscous flow at small Reynolds numbers, J. Phys. Soc. Jpn. 14 (1959) 527–532.
[8] H. Hasimoto, On the periodic fundamental solutions of the Stokes equations and their application to viscous flow past a cubic array of spheres, J. Fluid Mech. 5 (1959) 317–328.
[9] J. Happel, Viscous flow relative to arrays of cylinders, AIChE 5 (1959) 174–177.
[10] E.M. Sparrow, A.L. Loeffler, Longitudinal laminar flow between cylinders arranged in regular array, AICHE J. 5 (1959) 325–330.
[11] A.S. Sangani, A. Acrivos, Slow flow past periodic arrays of cylinders with application to heat transfer, Int. J. Multiphase Flow 8 (1982) 193–206.
[12] A.S. Sangani, C. Yao, Transport processes in random arrays of cylinders: II-viscous flow, Phys. Fluids 31 (9) (1988) 2435–2444.
[13] M. Sahraoui, M. Kaviany, Slip and no-slip boundary condition at interface of porous, plain media, Int. J. Heat Mass Transfer 37 (1994) 1029–1044.
[14] J. Vander Westhuizen, J.P. Du Plessis, An attempt to quantify fiber bed permeability utilizing the phase average Navier-Stokes equation, Composites 27A (1996) 263–269.
[15] M. Hellou, J. Martinez, M. El Yazidi, Stokes flow through microstructural model of fibrous media, Mech. Res. Commun. 31 (2004) 97–103.
[16] M.P. Sobera, C.R. Kleijn, Hydraulic permeability of ordered and disordered single-layer arrays of cylinders, Phys. Rev. 74 (2006) 036302-1–036302-10.
[17] M.M. Tomadakis, S.V. Sotirchos, Transport properties of random arrays of freely overlapping cylinders with various orientation distributions, J. Chem. Phys. 98 (1993) 616–626.
[18] M. Avellaneda, S. Torquato, Rigorous link between fluid permeability, electrical conductivity, and relaxation times for transport in porous media, Phys. Fluids 11 (1991) 2529–2540.
[19] C.P. Kyan, D.T. Wasan, R.C. Kinter, Flow of single-phase fluids through fibrous beds, Indust. Eng. Chem. Fundam. 9 (1970) 596–603.
[20] O.P. Bergelin, G.A. Brown, H.L. Hull, F.W. Sullivan, Heat transfer and fluid friction during viscous flow across banks of tubes: III – a study of tube spacing and tube size, ASME Trans. 72 (1950) 881–888.
[21] A.A. Kirsch, N.A. Fuchs, Studies on fibrous aerosol filters – II. Pressure drops in systems of parallel cylinders, Ann. Occup. Hyg. 10 (1967) 23–30.
[22] T.A.K. Sadiq, S.G. Advani, R.S. Parnas, Experimental investigation of transverse flow through aligned cylinders, Int. J. Multiphase Flow 21 (5) (1995) 755–774.
[23] B. Khomami, L.D. Moreno, Stability of viscoelastic flow around periodic arrays of cylinders, Rheol. Acta 36 (4) (1997) 367–383.
[24] W.H. Zhong, I.G. Currie, D.F. James, Creeping flow through a model fibrous porous medium, Exp. Fluids 40 (2006) 119–126.
[25] L. Skartsis, J.L. Kardos, The Newtonian permeability and consolidation of oriented carbon fiber beds, in: Proceedings of American Society of Composites Technical Conference, 1990, pp. 548–556.
[26] G.W. Jackson, D.F. James, The permeability of fibrous porous media, Can. J. Chem. Eng. 64 (1986) 364–374.
[27] B.T. Astrom, R.B. Pipes, S.G. Advani, On flow through aligned fiber beds and its application to composite processing, J. Compos. Materials 26 (9) (1992) 1351–1373.
[28] M. Bahrami, M.M. Yovanovich, J.R. Culham, Effective thermal conductivity of rough spherical packed beds, Int. J. Heat Mass Trans. 49 (2006) 3691–3701.

[29] E. Sadeghi, M. Bahrami, N. Djilali, Analytical determination of effective thermal conductivity of PEM fuel cell gas diffusion layers, J. Power Source 179 (1) (2008) 200–208.
[30] A. Szaniawski, Z. Lipnicki, Heat transfer to longitudinal laminar flow between thin cylinders, Int. J. Heat Mass Transfer 51 (2008) 3504–3513.
[31] T.M. Jeng, S.C. Tzeng, A semi-empirical model for estimating permeability and inertial coefficient of pin-fin heat sinks, Int. J. Heat Mass Transfer 48 (2005) 3140–3150.
[32] F.M. White, Viscous Fluid Flow, McGraw-Hill, New York, 1984.
[33] R.K. Shah, A.L. London, Laminar flow forced convection in ducts, Academic Press, 1978.
[34] M.M. Yovanovich, A general expression for predicting conduction shape factors, AIAA, Thermophys. Space Craft Control 35 (1974) 265–291.
[35] M.M. Yovanovich, New Nusselt and Sherwood numbers for arbitrary isopotential bodies at near zero Peclet and Rayleigh numbers, AIAA 22nd Thermophysics Conference, Honolulu, Hawaii, 1987.
[36] M. Bahrami, M.M. Yovanovich, J.R. Culham, Pressure drop of laminar, fully developed flow in microchannels of arbitrary cross-section, ASME J. Fluid Eng. 128 (2006) 1036–1044.
[37] M. Bahrami, M.M. Yovanovich, J.R. Culham, A novel solution for pressure drop in singly connected microchannels of arbitrary cross-section, Int. J. Heat Mass Transfer 50 (2007) 2492–2502.